

Support effects of nickel on activated carbon as a catalyst for vapor phase methanol carbonylation

Andrei S. Merenov, Amy Nelson, Martin A. Abraham *

Department of Chemical and Environmental Engineering, 2801 W. Bancroft, Toledo, OH 43606-3390, USA

Abstract

Nickel supported on activated carbon can be used for the vapor phase carbonylation of methanol, producing methyl acetate and acetic acid as products. In contrast to previous reports, a strong influence of the support on the performance of the catalyst, in terms of both activity and stability, was observed in the current study. The effect appears to be related to the pore size distribution of the support. Catalysts prepared on large pore activated carbons are less active than catalysts prepared on smaller pore activated carbons but show no deactivation over time on stream. The mechanism of deactivation appears to be consistent with a strong adsorption of methanol and reaction products that plugs the catalyst pores and leads to increasingly strong diffusion limitations with time on stream. ©2000 Elsevier Science B.V. All rights reserved.

1. Introduction

The current technology for production of acetic acid and methyl acetate is mainly based on the low pressure carbonylation or Monsanto process [1]. The process employs liquid phase reaction catalyzed by soluble rhodium salt. The presence of a halide promoter, preferably iodomethane, is essential for the process. The process is highly effective. According to the data reported by Stanford Research Institute (SRI) [1], conversion of methanol to the goal products is 50% in single pass and reaches 90% of total conversion after recycle; conversion of carbon monoxide is 83.3%. The residence time required to achieve these conversions is approximately 30 min [1]. Selectivity of methanol conversion to acetic acid is up to 95%.

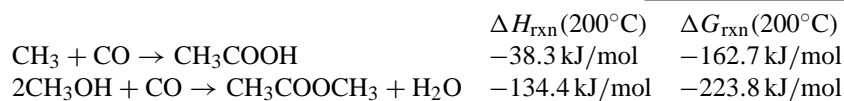
Although the process is highly effective, it does have certain disadvantages. The homogeneous reaction sys-

tem includes catalyst, catalyst promoter, methanol, acetic acid, methyl acetate and water. The latter is used as the solvent for the catalysts, creating a multiphase reaction system. According to the estimation of SRI [1] water/acetic acid ratio in the system is approximately 0.5. The use of such a system requires a sophisticated separation train. The separation section of the process includes four columns in order to separate non-reacted methanol and carbon monoxide, promoter and catalyst, water, and heavy ends. Water is separated in the third and the largest column of the separation train. Switching to a heterogeneous process and excluding water from the reaction system eliminates this column. The size and energy consumption of the first two columns will also be reduced due to elimination of the ballast water from the reaction system.

As an alternative to the liquid phase process, several research groups have studied possible catalysts that could be employed for heterogeneous vapor phase methanol carbonylation [2–5]. Nickel on activated carbon catalyst was reported as highly effective and stable. The reaction produces two major products;

* Corresponding author. Tel.: +1-419-530-8092;
fax: +1-419-530-8086
E-mail address: mabraham@eng.utoledo.edu (M.A. Abraham)

acetic acid and methyl acetate, with the latter typically formed in higher yield. The reactions can be described according to the following stoichiometric equations



Nickel supported on other materials (graphite carbon black, silica and alumina) has lower activity for both reactions and leads to the formation of other byproducts [2]. It is generally agreed that activated carbon has an important role in determining the activity, selectivity and stability of Ni/activated carbon catalyst. However, modification of the activated carbon by oxidation and subsequent defunctionalization was not effective for improvement of the properties of Ni/activated carbon catalysts [6]. Unfortunately, that research was done with experimental activated carbons that had significantly smaller surface area (350–820 m²/g) than commercially available activated carbons (950 m²/g and higher). Little additional research has been reported on the use and effect of commercially available activated carbon as a support for nickel catalysts employed for methanol carbonylation.

The goal of the present research is to study the influence of the properties of commercially available activated carbons on the activity and stability of Ni on activated carbon as a catalyst for vapor phase carbonylation of methanol.

2. Experimental

Catalyst samples were prepared in our laboratory and tested in an experimental packed bed reactor according to the procedures described below.

2.1. Catalyst preparation

Five catalysts listed in Table 1 were prepared using commercially available activated carbons. Darco brand activated carbon was purchased from Aldrich. The other activated carbons were obtained from Calgon Carbon Co. All activated carbons were used as received.

Each catalyst was prepared by impregnation of Nickel acetate tetrahydrate from organic solution followed by drying in flowing nitrogen at 100°C and

overnight reduction in flowing hydrogen at 200°C. The detailed procedure of the catalyst preparation was described in the previous work of the authors [7].

The particle size of all tested catalyst was 40–60 mesh (0.250–0.420 mm). In case of Catalyst 5, the support was crushed to this size from the material with larger particles provided by the manufacturer. The pore size distributions of activated carbons obtained from Calgon Carbon, as provided by the manufacturer, are shown in Fig. 1. These data clearly show that activated carbons Centaur and BPL have very similar pore size distribution with pore size significantly smaller than in case of activated carbons PCB and MRX-P. Estimation of the average pore size from the apparent density of the solid, indicated in Table 1, confirms the marked contrast in pore size and is in reasonable agreement with the pore size distributions shown in Fig. 1.

The surface area of fresh activated carbons obtained from Calgon Carbon and measured in our laboratory was very close to the specification provided by the manufacture. The deviation in the range of 10% might be explained by the variability of the physical properties of activated carbons from batch to batch and the error in our measurements. Except for the Centaur activated carbon (Catalyst 4), deposition of nickel resulted in a decrease in surface area of between 10 and 20%.

Nickel dispersion was measured for catalysts prepared on PCB and Centaur activated carbons using hydrogen adsorption at room temperature. Dispersion values of 0.137 and 0.025 were obtained for Catalysts 3 and 4, respectively. These low dispersion values suggest relatively large nickel particles distributed non-uniformly on the surface of the support.

2.2. Test program

Catalysts were tested in a glass packed bed continuous flow differential reactor at atmospheric pressure. Prior to each experiment, the tested catalyst was preheated to an initial temperature of 200°C in the reactor in a stream of nitrogen, after which the feed stream was introduced. The mixture of methanol and

Table 1
Summary of physical properties of tested catalysts.

Catalyst support	Ni load, wt. %	Catalyst load in reactor, g	Surface area of support (specified), m ² /g	Average pore diameter (estimated), Å	Surface area of support (measured), m ² /g	Surface area of catalyst, m ² /g
1. Darco	3.56	0.3723			1192	865
2. MRX-P	3.49	0.3699	900	29.2	924	759
3. PCB	3.89	0.3734	1055	22.3	1150	985
4. Centaur HSV	3.44	0.3692	1093.6	7.8	1014	1208
5. BPL	3.45	0.3714	1275	12.4	1148	1114

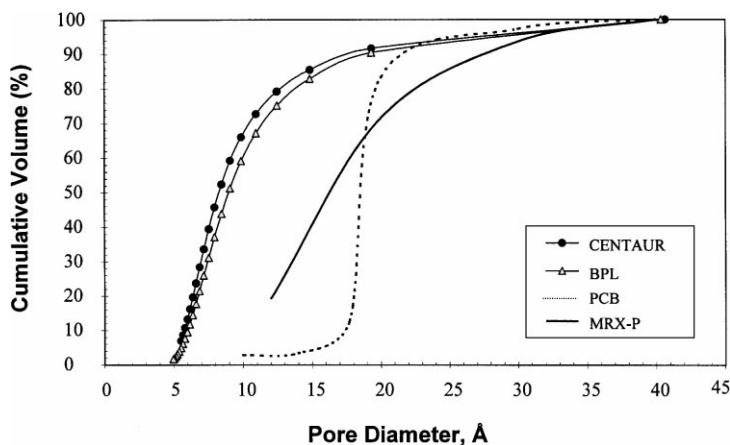


Fig. 1. Pore size distribution of activated carbon supports, as reported by the manufacturer.

iodomethane was injected into the system by a peristaltic pump. The analysis of the inlet and outlet composition was done with an online Dycor 200 M residual gas analyzer (mass spectrometer). The instrument was calibrated in the range of the observed concentration with pure chemicals purchased from Aldrich. A computer program for step by step deconvolution of the mass spectral peaks was written for quantitative analysis of the reactor inlet and outlet composition.

We utilized a five-stage catalyst test program to evaluate the performance of the catalysts. The feed composition, temperature and duration of each stage are summarized in Table 2. All the experiments were run at atmospheric pressure. During the first stage of the test program, the catalyst was on stream for 12 h at a constant temperature of 200°C. The residence time was approximately 0.25 s. The catalyst weight/flow rate ratio was 0.55 g_{cat} h/mol. During the second stage hydrogen was introduced at the rate of 10 ml/s for 6 h. After that hydrogen was shut down and the system returned to the previous operating condition for 2 h in order to return to a steady state. The thermal stabil-

ity of the catalysts was tested in the third stage of the experiment. The temperature of the reactor was raised from 200 to 290°C at a constant rate of 1°C/min. After that the temperature of the reactor was returned to the initial temperature of 200°C. Finally, all catalysts except Catalyst 4 were re-reduced during 15 h in a stream of nitrogen/hydrogen mixture. The temperature of the secondary reduction was 200°C. After the re-reduction, the catalysts were tested an additional 6 h at the same conditions as in Stage 1.

3. Results

Methyl acetate and acetic acid were the only products observed for the reaction. For all experiments, the yield of methyl acetate of approximately 0.02 was significantly higher than the acetic acid yield of approximately 0.005. Here, yield is defined as the flowrate of the product relative to the inlet flowrate of methanol. The observed product spectrum is consistent with the reaction network proposed by Fujimoto et. al. [2] for

Table 2
Catalyst testing program

Stage	1	2	3	4	5
Name	Test of stability over time on stream	Test for effect of hydrogen in feed	Test for thermal stability	Secondary reduction	Test of effect of secondary reduction
Duration (h)	12	6	~1.5	15	6
Temperature (°C)	200	200	200–300 ramp 1°C/min	200	200
	Feed composition (mol%)				
Carbon monoxide	87	86.1	87		87
Methanol	12	11.8	12		12
Iodomethane	1	0.99	1		1
Hydrogen		1.11		15	
Nitrogen				85	

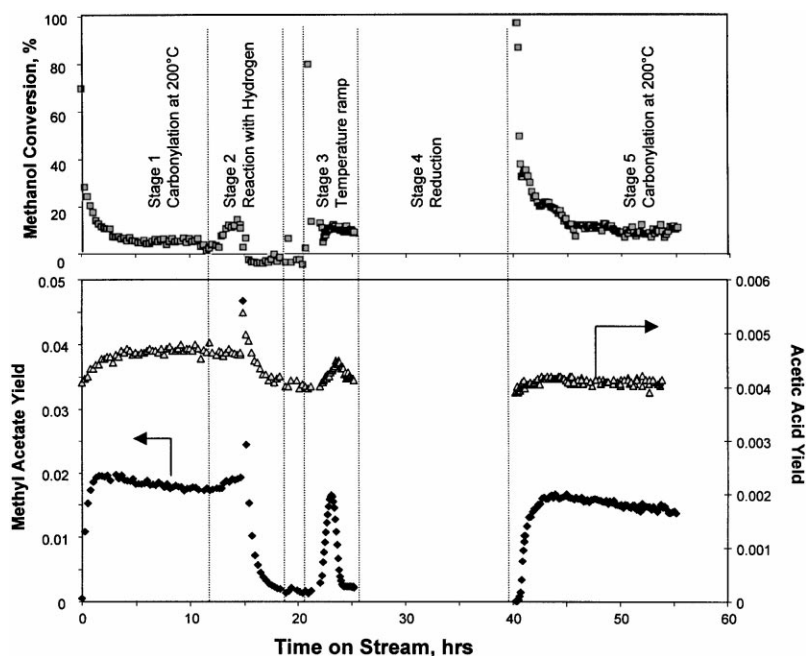


Fig. 2. Conversion and product yield behavior relative to time on stream and reaction conditions for nickel supported on BPL activated carbon.

a similar type of catalyst, who suggested that methyl acetate is the primary product and acetic acid is the secondary product. The low observed yields indicate the differential nature of the experiments and are consistent with the short residence time.

The behavior of Catalyst 5 over time is shown in Fig. 2 and was representative of all catalysts tested during the experimental program. Fig. 2a shows the methanol conversion and Fig. 2b reports the yield of

the observed products. The results obtained for each stage of the test program are described below.

3.1. Stage 1: catalyst activity and stability over time on stream

Methyl acetate yield reached a maximum of approximately 0.02 after an initial induction period of 2 h. This was followed by a relatively slow deactiva-

Table 3
Change of acetic acid and methyl acetate yields over time on stream. The first stage of the experimental program

Catalyst/support	Methyl acetate yield			Acetic acid yield		
	After 2 h	Steady state	Change (%)	After 2 h	Steady state	Change (%)
1. Darco	0.017	0.014	−17.64	0.0045	0.0043	−4.44
2. MRX-P	0.011	0.011	0.00	0.0043	0.0042	−2.35
3. PCB	0.004	0.004	0.00	0.0042	0.0041	−2.38
4. Centaur HSV	0.021	0.017	−19.05	0.0048	0.0053	10.42
5. BPL/crushed	0.020	0.017	−15.00	0.0045	0.0048	6.67

tion, during which time, the yield decreased to approximately 0.017. The yield of acetic acid was lower by nearly an order of magnitude, but remained at a constant value during the first stage of the experimental program. Fig. 2a shows that the conversion of methanol after the induction period was relatively constant and varied in the range of 4.5–6.5%. The high initial values of methanol conversion are consistent with strong adsorption of methanol on the fresh catalyst. CH₃ group balance performed for the steady state portion of Stage 1 reveals that greater than 85% of the reacted methanol was recovered in the observed products, the loss of methanol is likely a result of errors in the measurement of compositions of the inlet and outlet streams.

Methyl acetate and acetic acid yields that were observed after the induction period (2 h on stream) are compared with the values observed after 12 h on stream in Table 3 for each of the tested catalysts. Catalysts prepared on activated carbon with average pore size less than 10 Å (Catalysts 1, 4, and 5 prepared on Darco, Centaur and BPL activated carbon) had substantially higher yields of methyl acetate at 200°C than Catalysts 2 and 3 immediately following the induction period. However, the yield of methyl acetate remained constant over time for the less active Catalysts 2 and 3 (support MRX-P and PCB) prepared on the supports with larger pore sizes. Catalysts 4 and 5, which had the highest activity, also showed the greatest decrease in methyl acetate yield over time.

On the other hand, it was observed that the yield of acetic acid after 2 h on stream was approximately the same for all five catalysts. While a slight decrease in the acetic acid yield was observed for the catalysts produced on the large pore activated carbons, a small increase in acetic acid yield was observed for the catalysts produced on the small pore supports.

3.2. Stage 2: effect of hydrogen

Fig. 2a and b indicate that the introduction of hydrogen in the feed stream resulted in a short dramatic increase of acetic acid and methyl acetate yields and methanol conversion. The increase of the yields was followed by a relatively fast decrease in the catalyst activity. This observation is consistent with the theory that hydrogen competes favorably with both reactants and products for adsorption sites. Thus, adsorbed products are removed from the catalyst surface and adsorption of reactants is inhibited. The negative values of methanol conversion during the latter part of the second stage also support this hypothesis. After reaching a new steady state, the yields of both methyl acetate and acetic acid were substantially below the values observed when hydrogen was not present in the feed (end of Stage 1). After stopping H₂, Catalyst 5 did not regain activity. This result was not general, however, as several other tested catalysts did return to the yields achieved during the first stage of the program.

The results of the second stage of the experimental program are further described in Table 4. In all cases, hydrogen was observed to remove the reactants and the products from the surface of the catalysts, as evidenced by the short dramatic increase in the concentration of methyl acetate, acetic acid, methanol and methyl iodide in the outlet stream. Over the next 3 h the system reached a new steady state. Data presented in Table 4 show steady state yields of methyl acetate and acetic acid that have been achieved after 12 h on stream (first stage of the experimental program) and steady state yields that were observed after 6 h on-stream with hydrogen. The data clearly show that Catalysts 1, 4 and 5 prepared with activated carbon with smaller pores all had lower activity in the presence of hydrogen while Catalysts 2 and 3 showed slight activity improvement.

Table 4
Change of acetic acid and methyl acetate yields due to the presence of H₂ in the feed stream. the second stage of the experimental program

Catalyst/support	Methyl acetate yield			Acetic acid yield		
	Stage 1, steady state	Stage 2, steady state	Change (%)	Stage 1, steady state	Stage 2, steady state	Change (%)
1. Darco	0.014	0.0020	−85.71	0.0043	0.0041	−4.65
2. MRX-P	0.011	0.0120	9.09	0.0042	0.0049	16.67
3. PCB	0.004	0.0047	17.50	0.0041	0.0047	14.63
4. Centaur HSV	0.017	0.0044	−74.12	0.0053	0.0044	−16.98
5. BPL/crushed	0.017	0.0020	−88.24	0.0048	0.0040	−16.67

Table 5
Summary of thermal stability data and resulting estimates of activation energy

Catalyst/support	Experimental method ^a	Critical temperature (°C)	Maximum methyl acetate yield	Apparent activation energy, (kJ/mol)
1. Darco	1	237.0	0.005	27.6 ± 3.4
2. MRX-P	1	263.1	0.026	41.1 ± 2.6
3. PCB	1	257.9	0.017	39.4 ± 2.8
4. Centaur HSV	1	278.0	0.023	7.5 ± 3.3
5. BPL	1	257.5	0.017	19.7 ± 2.0
3. PCB/80–100 mesh	2	258.2	0.049	42.3 ± 5.8
4. Centaur HSV	2	269.1	0.064	33.2 ± 3.3
5. BPL	2	248.7	0.019	34.9 ± 6.4

^a Experimental Method 1 corresponds to Stage 3 of standard test program, following 12 h at 200°C, 6 h at 200°C with hydrogen, and 2 h at 200°C to achieve a new steady state. Experimental Method 2 corresponds to temperature program following 2 h at 200°C to achieve a steady state.

The decrease of the activity of Catalysts 4 and 5 can not be explained by loss of nickel since these catalysts returned to their original activity after secondary reduction in hydrogen.

It is necessary to mention that the decrease of the methyl acetate yield is significantly higher than that of acetic acid in the case of Catalysts 4 and 5, but that increase in the yields in the case of Catalysts 2 and 3 are approximately the same. This fact can not be explained only by the difference in the pore size distributions of the tested catalysts. The disproportional decrease of the yields of acetic acid and methyl acetate in case of Catalysts 4 and 5 might indicate the presence of different active sites on the surface of those catalysts. This hypothesis requires additional studies and will be addressed in future work.

3.3. Stage 3: test for thermal stability

The heating of Catalyst 5 up to 267.5°C during the third stage of the experimental program led to an increase in methanol conversion up to its maximum

value of 12.4% (Fig. 2a) as well as an increase in methyl acetate and acetic acid yields (Fig. 2b). Additional heating up to 290°C led to rapid loss of catalyst activity. Similar behavior for all catalysts was previously observed [7] and is reported in Table 5, in terms of the temperature at which the maximum yield of methyl acetate was observed. It was also shown that catalysts did not regain activity when returned to lower temperature.

The reaction rates of methyl acetate formation (calculated as the ratio of methyl acetate flowrate in the outlet stream to the amount of the catalyst loaded in the reactor) observed during this stage of the experiment are presented in Fig. 3 in the form of an Arrhenius plot. These data were then used to calculate apparent activation energies for methyl acetate formation as reported in Table 5. The activation energy of 39.4 and 41.0 kJ/mol for Catalysts 2 and 3 prepared on activated carbon with large pores were substantially larger than the values measured for Catalysts 4 and 5 (small pore size). This indicates a possibility of strong internal diffusion limitation for reaction over the small pore catalysts.

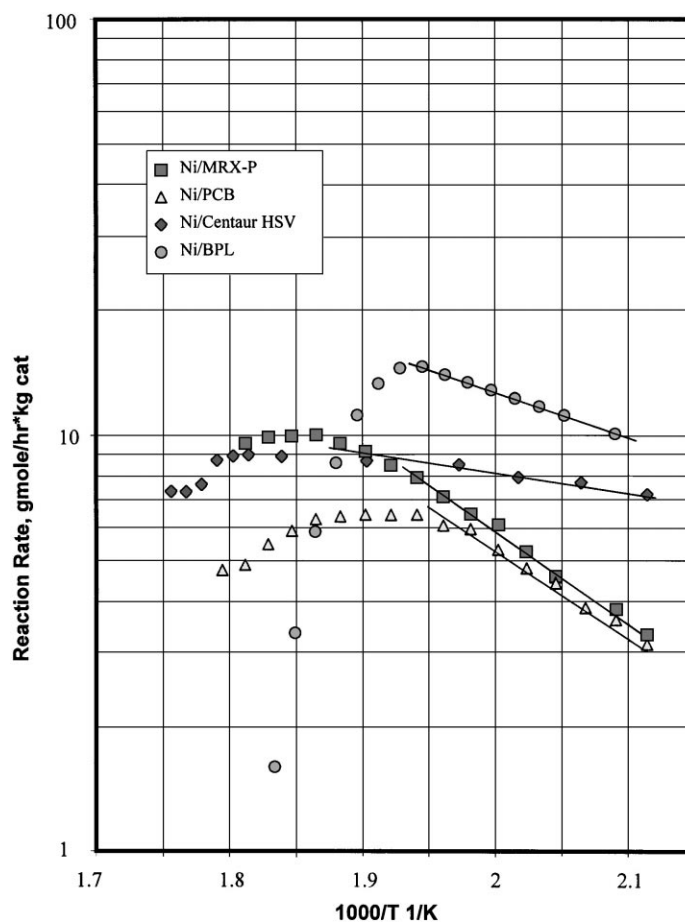


Fig. 3. Test for thermal stability. Third stage of experimental program.

The effect of the internal diffusion limitation on the apparent activation energy in the case of heterogeneous catalysts has been described elsewhere [8]. The quantitative effect is described by the classic equation of Weisz and Prater [8]

$$\frac{E_{\text{obs}}}{E} = 1 + \frac{1}{2} \frac{d(\ln \eta)}{d(\ln \phi)}$$

where E and E_{obs} are intrinsic and observed activation energies, η is overall effectiveness factor and ϕ is the Thiele modulus. The Thiele modulus is dependent on the diffusivity within the catalyst pores. Within the range of pore sizes associated with the activated carbons used in this study, the diffusivity is most likely of the Knudsen or configurational type, which is a function of the effective pore diameter. As a result, the ob-

served activation energy may be substantially reduced due to strong internal diffusion limitations. Since the Thiele modulus is also a function of catalyst particle size, the observed activation energy will also be dependent on particle size in the region of strong diffusion limitations.

Thus, to test for internal diffusion limitation, Catalyst 3 (support PCB) originally 40–60 mesh was crushed to size 80–100 mesh (0.149–0.077 mm). Fresh crushed catalyst was loaded in the reactor and after the end of the induction period (2 h) was heated at the rate 1°C/min. The results for the two particle sizes are compared in Fig. 4 and the calculated apparent activation energies are given in Table 5. It can be seen from the results there is no significant difference between the values of apparent activation

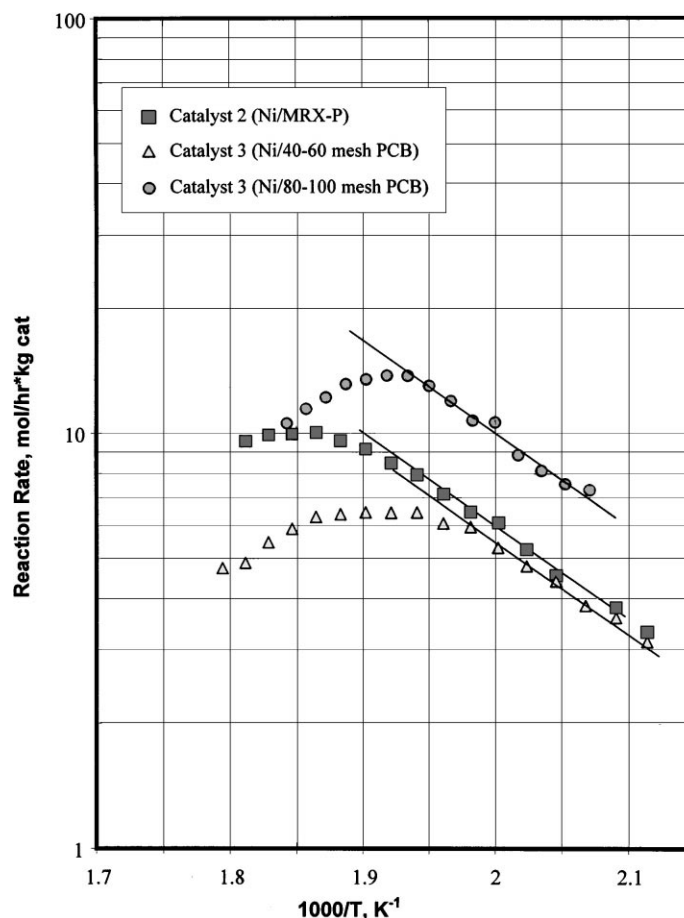


Fig. 4. Test for internal diffusion limitations.

energy in these cases (39.38 ± 2.76 and 42.34 ± 5.81). However, the reaction rate for the crushed catalyst is observed to be approximately twice that of the bulk material, suggesting significant internal mass transfer limitations exist in these catalysts.

3.4. Stage 4: effect of secondary reduction

The heating of the catalyst was followed by reduction of the catalyst in hydrogen/nitrogen flow and then return to the reaction conditions of Stage 1. In the case of Catalyst 5 (as shown in Fig. 2), the initial methyl acetate yield was the same as the steady state value from Stage 1, however, a small decrease in acetic acid yield relative to Stage 1 was observed. The steady state methanol conversion was approximately the same as

that observed at the end of the third stage of the experimental program. In the previous study of the authors' [7] it was shown that heating the catalysts above a certain critical temperature led to a loss of the catalysts activity. Here it is observed that secondary reduction with H_2 allows the restoration of catalyst activity to that observed before heating.

In general, the secondary reduction did not influence methyl acetate and acetic acid yield for the studied catalysts. Practically, all tested catalysts gained back activity to the steady value at the end of Stage 1. Thus, it is clear that any loss of catalyst activity during previous experiments was not because of the nickel loss from the surface of the tested activated carbons. The observed deactivation might be explained either by coke formation or by deposition of the products of the

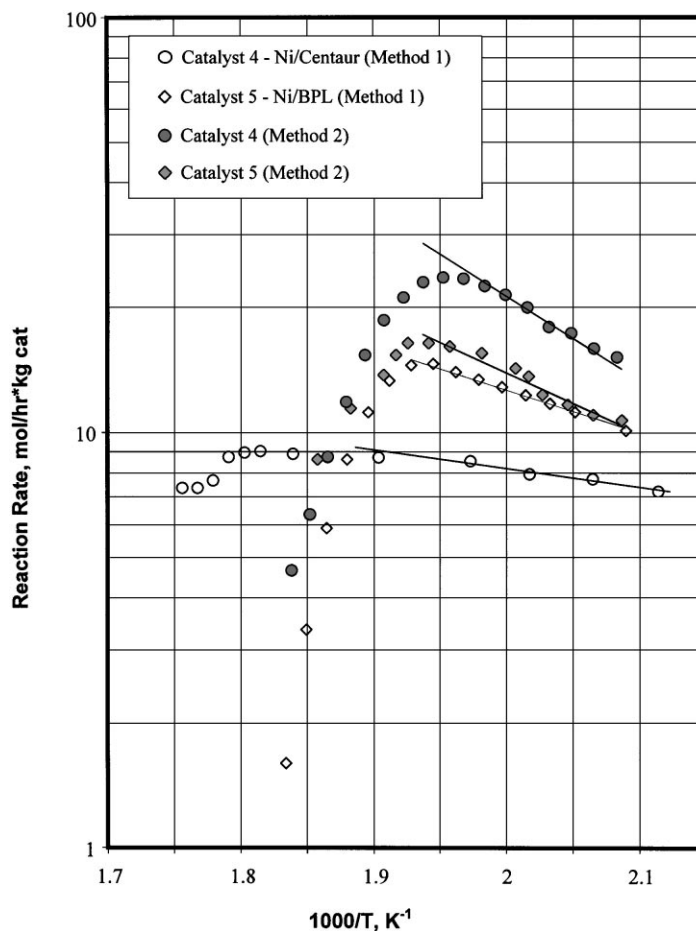


Fig. 5. Increase of internal diffusion limitations for Catalyst 4 (Centaur activated carbon) and Catalyst 5 (BPL activated carbon).

reaction on the surface of the catalysts, which are then stripped off by hydrogen during the reduction step. A similar effect was observed during the second stage of the experimental program when hydrogen was added in the feed.

4. Discussion

The observed behavior of tested catalysts during the first and second stages of experimental program indicates that the reactants and the products of the reaction strongly absorb within the pores of the catalysts. In all cases, the addition of hydrogen to the feed resulted in a large generation of reaction products that was in excess of the amount that could be produced

from conversion of all of the feed methanol. Furthermore, the continued feed of hydrogen eventually leads to methanol conversion that is less than zero, suggesting removal of methanol that had previously been adsorbed on the catalyst surface.

Hydrogen added in the feed stream not only removes adsorbed species but also alters the product selectivity. In the presence of hydrogen, acetic acid is observed to be the preferred product, having a higher yield than methyl acetate. One of the possible explanations of this fact might be the presence of adsorbed intermediate CH_3COO group. The intermediate group can produce methyl acetate by reaction with methanol and acetic acid by reaction with hydrogen.

The deactivation of the catalysts produced on activated carbons with small average pore size is also

attributed to the accumulation of adsorbed species within the catalyst pores. A closer analysis of the molecular dimensions provides some justification for this hypothesis. Catalyst 4 and 5, prepared on activated carbons with average pore diameters less than 15 Å, were observed to deactivate over time, whereas Catalysts 2 and 3, prepared with activated carbons of average pore diameter greater than 20 Å only experienced minimal deactivation. We first note that the estimated molecular size of the reaction products, acetic acid and methyl acetate, is on the order of 5 Å. The estimated average pore diameter for Centaur activated carbon is slightly less than 8 Å. Even methanol, with an estimated molecular size of approximately 4 Å represents a significant fraction of the average pore diameter of the Centaur activated carbon. As a result, an adsorbed molecule would significantly decrease the effective pore diameter through which a molecule could diffuse. As the mass transfer resistance becomes increasingly large, the conversion of methanol should decrease and the observed activation energy should approach a small value consistent with the temperature dependence of the mass transfer coefficient.

The proposed deactivation model requires that 'fresh' catalysts have substantially higher activation energies than the catalysts that have been on-stream for an extended period. In order to investigate this issue further, samples of the catalysts prepared with the small pore activated carbons were tested for thermal stability after the end of induction period (2 h on stream) but before reaction with hydrogen (designated as Method 2). The results of the test are presented in Fig. 5 in the form of an Arrhenius plot and the calculated activation energies of methyl acetate formation calculated from the data are presented in Table 5. For both catalysts, the apparent activation energies were significantly higher in the case of 'fresh' catalysts.

Comparison of the reaction rates reveals that for the catalyst prepared on Centaur activated carbon (average pore diameter of approximately 8 Å) the rate for 'fresh' catalyst was more than twice that of the deactivated catalyst. On the other hand, the rate of reaction over the catalyst prepared on BPL activated carbon (12.4 Å) was only slightly lower when measured after deactivation than that measured using Method 2. This result would appear to validate our hypothesis that internal mass transfer has a significant role in controlling both the rate of reaction and the rate of deactivation.

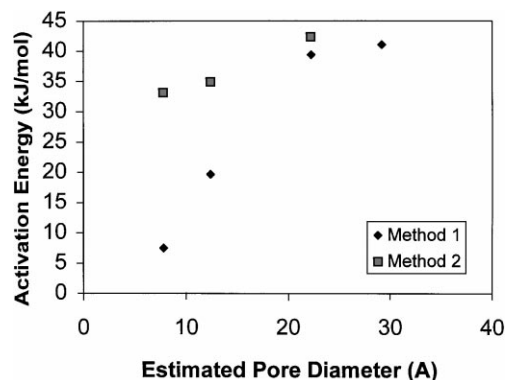


Fig. 6. Correlation of the observed activation energy with the estimated average pore diameter of the catalyst support.

Fig. 6 provides a more complete comparison of the observed activation energy for all tested catalysts as a function of the estimated average pore diameter. We note that the observed activation energy increases approximately linearly with the estimated average pore size, the result expected when mass transfer limitations are severe. We also note fresh catalysts had higher activation energies than the deactivated catalysts, regardless of the pore size. Finally, we can observe that the decrease in activation energy becomes increasingly less significant as the average pore size of the support increases. This is again consistent with the proposed deactivation mechanism. For the Centaur catalyst, with an average pore size of less than 8 Å, an adsorbed molecule of 4 Å in diameter occupies approximately 50% of the pore diameter, making it impossible for two molecules to pass within a small pore. However, for the large pore activated carbons, the molecular size of the products is less than 20% of the average pore diameter and adsorption of the products creates only a small change in the mass transfer resistance within the catalyst pores.

5. Conclusions

Nickel on activated carbon is effective for the carbonylation of methanol to methyl acetate and acetic acid. Under carbonylation conditions, methyl acetate is the preferred product; inclusion of hydrogen in the feed changes the selectivity of the reaction in favor of acetic acid. The observed product spectrum suggests

a mechanism that involves formation of a strongly adsorbed CH_3COO surface intermediate.

Catalysts prepared on activated carbons with small average pore size are initially more active than those prepared on large pore supports but deactivate with time. The mechanism of deactivation is proposed as accumulation of reactants in the pores of the catalysts. This proposed mechanism is consistent with the observation of a large increase in product formation immediately following addition of hydrogen to the feed, and the substantially reduced activation energy and reaction rates observed for deactivated catalysts produced on small pore activated carbons.

Acknowledgements

The authors would like to express appreciation to Calgon Carbon Corporation for providing the samples

of activated carbons and to Guild Associates, Inc. for financial support of the catalyst research program.

References

- [1] SRI Report 37 A, Acetic Acid and Acetic Anhydride, Menlo Park, California, 1973.
- [2] K. Fujimoto, K.K. Omata, T. Shikada, H. Tominaga, Industrial chemicals via C1 processes, in: Darryl R. Fahey (Ed.), ACS Symposium Series 328, American Chemical Society, Washington, DC (1987).
- [3] T.-C. Liu, S.-J. Chiu, *Ind. Eng. Chem. Res.* 33 (1994) 488.
- [4] T.-C. Liu, S.-J. Chiu, *Ind. Eng. Chem. Res.* 33 (1994) 1674.
- [5] T. Yashima, Y. Orikasa, N. Takashi, N. Hara, *J. Catal.* 59 (1979) 53.
- [6] S. Bischoff, H.-E. Maneck, H. Preiss, K. Fujimoto, *J. Appl. Catal.* 75 (1991) 45.
- [7] A.S. Merenov, M.A. Abraham, *Catal. Today* 40 (1998) 397.
- [8] G.F. Froment, K.B. Bischoff, in: *Chemical Reactor Analysis and Design*, 2nd edn., Wiley, New York, 1990.